The CAPOS mutation in *ATP1A3* alters Na/K-ATPase function and results in auditory neuropathy which has implications for management

Lisbeth Tranebjærg*[,1,2,3] Nicola Strenzke*[4] Sture Lindholm[5] Nanna D. Rendtorff[2] Hanne Poulsen[6] Himanshu Khandelia[7] Wojciech Kopec[,7,8] Troels J. Brünnich Lyngbye[9] Christian Hamel†[10,11,12] Cecile Delettre[11,12] Beatrice Bocquet[10,11,12] Michael Bille[13] Hanne H. Owen[14] Toke Bek[15] Hanne Jensen[16] Karen Østergaard[17] Claes Möller[18] Linda Luxon[19] Lucinda Carr[20] Louise Wilson[21] Kaukab Rajput[22] Tony Sirimanna[23] Katherine Harrop-Griffiths[24] Shamima Rahman[25] Barbara Vona[26] Julia Doll[26] Thomas Haaf[26] Oliver Bartsch[27] Hendrik Rosewich[28] Tobias Moser [29] Maria Bitner-Glindzicz*[,21, 25]

* These authors contributed equally to the manuscript.

[1] Department of Otorhinolaryngology, Head & Neck Surgery and Audiology, Rigshospitalet/Bispebjerg, Copenhagen, Denmark
[2] Department of Clinical Genetics/The Kennedy Center, University Hospital, Copenhagen, Denmark
[3] Institute of Clinical Medicine, University of Copenhagen, Copenhagen, Denmark
[4] Auditory Systems Physiology Group, InnerEarLab, Department of Otolaryngology, University Medical Center, Göttingen, Germany
[5] ENT-department, County Hospital Kalmar, Sweden
[6] Institute of Biomedicine, University of Aarhus, DK-8000 Aarhus, Denmark
[7] MEMPHYS – Center for Biomembrane Physics, University of Southern Denmark, Denmark
[8] Computational Biomolecular Dynamics Group, Max Planck Institute for Biophysical Chemistry, Göttingen, Germany
[9] Pediatric Department, Aarhus University Hospital, Denmark
[10] Maladies Sensorielles Genetiques, CHRU, Montpellier, France;
[11] INSERM U1051, Institute for Neurosciences of Montpellier, France;
[12] Universite Montpellier, France
[13] Department of Otorhinolaryngology, Head & Neck Surgery and Audiology, Rigshospitalet/Gentofte Hospital, Hellerup, Denmark
[14] Department of Audiology, Aarhus University Hospital, Aarhus, Denmark
[15] Department of Ophthalmology, Aarhus University Hospital, Aarhus, Denmark
[16] Eye Department Glostrup Hospital/Rigshospitalet, The Kennedy Centre, Glostrup, Denmark
[17] Department of Neurology, Aarhus University Hospital and University of Aarhus, Aarhus, Denmark
[18] Audiological Research Centre, Faculty of Medicine and Health, Örebro University, Örebro, Sweden

[19] Department of Neurotology, National Hospital for Neurology, Queen Square, London WC1N 3BG, UK

[20] Department of Neurology, Great Ormond Street Hospital for Children NHS Foundation Trust, London WC1N 3JH, UK

[21] Department of Clinical Genetics, Great Ormond Street Hospital for Children NHS Foundation Trust, London WC1N 3JH, UK

[22] Cochlear Implant Department, Great Ormond Street Hospital for Children NHS Foundation Trust, London WC1N 3JH, UK

[23] Department of Audiovestibular Medicine, Great Ormond Street Hospital for Children NHS Foundation Trust, London WC1N 3JH, UK

[24] Nuffield Hearing and Speech Centre, Royal National Throat Nose and Ear Hospital, London WC1X 8DA, UK

[25] Genetic and Genomic Medicine Programme, UCL Great Ormond Street Institute of Child Health, London WC1N 1EH, UK

[26] Institute of Human Genetics, Julius Maximilians University Würzburg, Würzburg, Germany

[27] Institute of Human Genetics, University Medical Centre, Johannes Gutenberg University Mainz, Langenbeckstrasse 1, Mainz, Germany

[28] Division of Pediatric Neurology, Department of Pediatric and Adolescent Medicine, University Medical Center, D-37075 Göttingen, Germany

[29] Institute for Auditory Neuroscience and InnerEarLab, University Medical Center, Göttingen, Germany

Corresponding Authors: Lisbeth Tranebjærg, Department of Clinical Genetics/The Kennedy Center, University Hospital, DK-2600 Glostrup, Denmark; E-mail: tranebjaerg@sund.ku.dk

And Maria Bitner-Glindzicz, Department of Clinical Genetics, Great Ormond Street Hospital for Children NHS Foundation Trust, London WC1N 3JH, UK and Genetic and Genomic Medicine Programme, UCL Great Ormond Street Institute of Child Health, London WC1N 1EH, UK; email: maria.bitner@ucl.ac.uk

Running title: Auditory Neuropathy caused by CAPOS syndrome

2

ABSTRACT

CAPOS (Cerebellar ataxia, Areflexia, Pes cavus, Optic atrophy and Sensorineural hearing impairment), is a rare clinically distinct syndrome caused by a single dominant missense mutation, c.2452G>A, p.Glu818Lys, in *ATP1A3*, encoding the neuron-specific alpha subunit of the Na+/K+-ATPase α3. Allelic mutations cause the neurological diseases Rapid Dystonia Parkinsonism (RDP) and Alternating Hemiplegia of Childhood (AHC), disorders which do not encompass hearing or visual impairment.

We present detailed clinical phenotypic information in 18 genetically-confirmed patients from 11 families (10 previously unreported) from Denmark, Sweden, UK and Germany indicating a specific type of hearing impairment - auditory neuropathy (AN). All patients were clinically suspected of CAPOS and had hearing problems. In this retrospective analysis of audiological data, we show for the first time that cochlear outer hair cell activity was preserved as shown by the presence of otoacoustic emissions and cochlear microphonic potentials, but the auditory brainstem responses were grossly abnormal, likely reflecting neural dyssynchrony. Poor speech perception was observed, especially in noise, which was beyond the hearing level obtained in the pure tone audiograms in several of the patients presented here.

Molecular modelling and *in-vitro* electrophysiological studies of the specific CAPOS mutation were performed. Heterologous expression studies of α3 with the p.Glu818Lys mutation affects sodium binding to, and release from, the sodium-specific site in the pump, the third ion binding site. Molecular dynamics simulations confirm that the structure of the C-terminal region is affected.

In conclusion, we demonstrate for the first time evidence for auditory neuropathy in CAPOS syndrome, which may reflect impaired propagation of electrical impulses along the spiral ganglion neurons. This has implications for diagnosis and patient management. Auditory neuropathy is difficult to treat with conventional hearing aids, but preliminary improvement in speech perception in some patients are encouraging for trying cochlear implantation in CAPOS patients.

Key words: optic atrophy, auditory neuropathy, aseptic encephalitis, *ATP1A3*, CAPOS syndrome

INTRODUCTION

CAPOS syndrome (OMIM 601338) is a rare but highly distinctive cause of hearing impairment, first described in a mother and two children in 1996 (Nicolaides 1996); seven further families and isolated cases (in total 22 patients) have been described subsequently (Demos et al 2014; Rosewich et al 2014; Heimer et al 2015; Potic et al 2015; Maas et al 2016). It is caused by one specific, dominant, missense mutation in the *ATP1A3* gene, on chromosome 19q13.2 (Demos et al 2014), encoding the neuron-specific alpha subunit of the Na+/K+-ATPase α3, while other mutations in the same gene cause neurological syndromes without hearing impairment or optic atrophy, namely Rapid Dystonia and Parkinsonism (RDP) and Alternating Hemiplegia of Childhood (AHC) (Dard et al 2015; Sweney et al 2015). CAPOS is thus clinically and molecularly distinct. The clinical picture is remarkable, characterized by sudden onset of cerebellar ataxia precipitated by a febrile illness in childhood. Episodes are often recurrent and they can involve extended periods of reduced consciousness, hypotonia, ataxia and loss of the ability to walk, which may take weeks or months to regain. Months or years later the patients experience progressive sensorineural hearing impairment, optic atrophy, loss of deep tendon reflexes, and in some subjects, pes cavus. Cognition and brain imaging are usually normal (Maas et al 2016). None of the previous reports have characterized the audiological phenotype to be an auditory neuropathy.

For all three allelic disorders, AHC, RDP and CAPOS, fever has been reported as a trigger, and several symptoms have been observed in all three groups, including ataxia, (asymmetric) dystonia, dysarthria, bradykinesia and abnormal ocular movements. For AHC, there are clear mutational hotspots with a majority of the patients having one of three residues affected, all in the transmembrane part of the protein at or close to the ion binding residues. In contrast, the RDP-causing mutations map more broadly onto the pump structure (Clausen et al, 2017). Effects on protein expression have been reported for RDP, but not AHC mutations (Heinzen et al, 2014).

The Na,K-ATPase establishes the steep gradients of sodium and potassium across animal cell membranes that are important for numerous processes, not least in neurons, where the firing of action potentials depends directly on the flow of these ions. In grey matter, it is estimated that as much as 75% of the energy produced in the brain is spent by the Na,K-ATPase (Attwell and Laughlin, 2001). A Na,K-ATPase consists of three subunits, the catalytic α and

4

two auxiliary subunits, β and FXYD, important for stability, trafficking and kinetic parameters (Geering et al, 2005). The α subunit has ten transmembrane helices that transport three Na^+ ions out of the cell and take up two K^+ ions at the expense of one ATP during each catalytic cycle (Fig. 1).

There are several isoforms of each of the subunits; there are three types of α subunit in brain of which α1 is broadly expressed, α2 is mostly in glia cells, and α3 is in neurons (Clausen et al 2017; Watts et al 1991; Schuth et al 2014). In the inner ear of rats, α3 was detected in the spiral ganglion neurons (SGNs) on hair cells, while α1 was detected in the hair cells themselves. (Schuth et al. 2014).

In the majority of cases sensorineural hearing impairment is caused by defects of auditory transduction (conversion of sound energy into electrical activity) and active amplification of cochlear vibrations by the electromotile outer hair cells (OHCs). Cochlear transduction and amplification can be directly reported by measuring sound emissions from the ear (otoacoustic emissions (Kemp 1978) or cochlear microphonics (the receptor potential generated by OHC). OAEs are absent when cochlear transduction and amplification fail, which makes them a useful screen for the majority of cases of congenital hearing impairment. In contrast, far less is known about hearing disorders affecting the auditory pathway beyond the OHCs, for example those affecting only inner hair cell (IHC) synapses, synaptic transmission to afferent spiral ganglion neurons (SGNs) or conduction of information by the auditory nerve to higher auditory centers (Rance and Starr 2015;Moser and Starr 2016). This type of hearing impairment is termed auditory neuropathy (AN) or auditory synaptopathy if synaptic sound encoding is affected. It is characterized by normal OHC amplification and the presence of OAEs and/or cochlear microphonics, but abnormal auditory nerve function, as measured by auditory brain stem responses (ABRs) and/or compound action potential by electrocochleography (CAP) (Rance and Starr 2015, Santarelli et al, 2015). ABRs require the synchronized activation of afferent SGNs by glutamate release at IHC ribbon synapses and intact propagation of spikes along the auditory pathway (Moser and Starr, 2016). Precise timing of neural activity is an important factor on which speech intelligibility and binaural hearing depend (Giraudet and Avan 2012).

5

Auditory neuropathy may be an isolated feature (non-syndromic) in some patients or part of a more widespread neuropathy or part of a syndrome disorder in others (Starr et al 1996). The distinction between AN and sensory (or cochlear) hearing impairment is critically important for diagnosis, prognosis and rehabilitation and there is growing evidence that AN underlies hearing dysfunction associated with several genetic and non-genetic diseases.

The combination of optic atrophy and 'sensorineural' hearing loss, coupled with known selective expression of *ATP1A3* in the spiral ganglion neurons of the inner ear (McGuirt and Schulte 1994; Watts et al 1991; Schuth et al 2014), indicate that the hearing loss in patients might not be due to hair cell dysfunction but to an auditory neuropathy instead. We describe 18 cases of CAPOS syndrome highlighting its unique clinical presentation, and provide evidence of an auditory neuropathy which has important implications for patient management. We model the specific mutation, p.Glu818Lys, in *ATP1A3* which causes CAPOS syndrome demonstrating effects which are different to mutations associated with RDP and AHC to try and better understand the reasons for its unique clinical presentation.

RESULTS

Clinical details of 18 patients with CAPOS syndrome are summarized in Tables 1 and 2 and in Supplementary material. Pedigrees of four familial cases and representative audiograms are shown in figures 2 and 3. All families showed the same recurrent heterozygous mutation in exon 18: c.2452G>A; p.Glu818Lys (supplementary Fig. S1).

Clinical histories are remarkably similar, and resemble earlier reports of CAPOS syndrome with episodes of reduced consciousness and ataxia, triggered by a febrile illness beginning suddenly in early childhood. Episodes were reminiscent of encephalitis and improved slowly over weeks or months with or without noticeable residual neurological deficit initially. Sometimes, definite but different pathogens were isolated and in case 9 three different pathogens were associated with three different episodes (raised mycoplasma titers, HPV6 infection and streptococcal throat infection). Episodes were often recurrent, and most episodes ceased in childhood but two patients experienced their last episode at or beyond 20 years of age. The single proband without episodes triggered by febrile illness (proband 18,

family 11) was diagnosed with 'episodic migraine' similar to the description by Potic et al (Potic et al 2015). Children were noted to have hearing impairment and visual dysfunction that were very slowly progressive (see Supplementary material). In 3 cases, hearing impairment was diagnosed before or at the same age as the first neurological episode (cases 3, 11 and 18) but in the other 15 cases, hearing impairment was diagnosed often years after the febrile episodes (1.5 – 11 years) and was not apparent immediately. Nine cases had clear nystagmus which often but not always persisted following improvement of the other symptoms. Interestingly, cases 1-7 demonstrated marked variability in their pure tone audiograms, showing occasional improvement.

Audiological data are summarized in Table 2. Six cases (cases 3, 4, 6, 16 ,17 ,18) had mild hearing loss, 8 had moderate (cases 1,2, 7, 9, 10 ,12 ,14 ,15) and 4 patients (cases 5, 8, 11, 13) had severe hearing loss. Hearing impairment tended to affect lower frequencies initially; it was progressive in 15 of the 18 cases (Table 2 and Fig. 3). In several cases, progression resulted in profound bilateral hearing loss. Some patients (cases 1, 2, 7 and 12) can only communicate with sign language (although this was not always the case) even though their pure tone audiogram shows a moderate to severe hearing loss. Their mode of communication reflects the very poor ability to understand speech even in quiet environment. Four patients (cases 9,11,15, 16) underwent cochlear implantation and some, particularly the children (cases 15 and 16), have gained significant benefit (See Supplementary Information, cases 15 and 16).

Hearing impairment was consistent with auditory neuropathy. Detailed audiological data are shown for case 17 in figure 4. Thirteen of the 15 patients tested, had OAEs; in two cases they were noted to be of particularly high amplitude (Fig. 4B, Fig. S2). The two cases (case 1 and case 13) without OAEs were aged 38 and 26 years and it is conceivable that OAEs had been present earlier but since disappeared as has been described for other types of auditory neuropathy. ABRs were markedly abnormal in all the 17 cases tested. Speech perception was often poor, especially in comparison with pure tone audiogram which showed only moderate or mild-moderate hearing loss in cases 15-18 (see Supplementary Information and Supplementary Figures 5 and 6). Fig.4 illustrates data for case 17, family 10 (Rosewich et al 2014). Pure tone audiogram shows symmetric, mild to moderate hearing loss (Fig. 4A). The discrimination of monosyllabic words in quiet was clearly impaired for conversational sound intensities (at 65dB 50% correct discrimination at the right ear; and 60% at the left ear, but

near normal at higher sound levels (80dB: 95%/100% at right /left ear). The speech recognition threshold in 65dB background noise (Oldenburger Sentence test, binaural) was at a signal to noise ratio of +0.5dB (Brand and Wagener, 2017). Despite the hearing impairment 86dB clicks readily elicited Transitory Evoked OAEs (TEOAE) (Figure 4B). Tone-evoked Distortion Product OAEs (DPOAEs) were present at higher amplitudes across all frequencies (Fig. 4D) indicating that the origin of the hearing impairment resides downstream of OHCs. We did not detect obvious ABRs (Fig. 4C and Supplementary Figs S2, S3, S4, S5, S6). Transtympanic electrocochleography (Figure 4C), which enables direct recordings of cochlear potentials showed the presence of cochlear microphonic potentials but much reduced (Fig. 4D). This indicates intact OHC function even in the low frequency apex of the cochlea, where the greatest hearing impairment is apparent in the pure tone audiogram.

To address the distinct effects of Glu818Lys on the $\alpha 3$ containing Na/K-ATPase, we expressed it with $\beta 1$ in *Xenopus laevis* oocytes. The 818 position is located at the cytoplasmic side of transmembrane helix 6 (Fig. 5A), where it forms a salt bridge with the backbone carbonyl of Arg930 (Fig. 5B), a residue known to stabilize the C-terminus (Morth et al. 2007; Poulsen et al. 2010). We therefore expected Glu818Lys to affect the C-terminal structure, which is critical for regulation of the Na^+-specific third ion binding site in the pump (Poulsen et al. 2010, Yaragatupalli 2009, Vedovato 2010). If the pump is expressed and functional, it will produce a steady-state current since one net charge is exported during each catalytic cycle, and this current will be sensitive to the pump-specific inhibitor ouabain. With Glu818Lys, a ouabain-sensitive steady-state current is measured (data not shown). In the absence of extracellular K^+, the pump will be restricted to binding and release of Na^+ on the extracellular side (Fig. 1). Since the third Na^+ is buried in the membrane, the membrane potential can shift the distribution of occluded (E1P) and open-to-the-outside (E2P) states, and the pre-steady-state currents from binding and release of the ion can be measured to determine this distribution (Holmgren et al 2000). We found that with Glu818Lys, the charge translocation is markedly left-shifted ($V_{0.5}$ shifted from -72 mV to -202 mV), reflecting that the equilibrium is shifted between the sodium-binding E1P state and the open-to-the-outside E2P state towards E2P, i.e. Glu818Lys releases extracellular sodium more readily than the wild type pump (Fig. 6). The rate of sodium release is also accelerated compared to wild type $\alpha 3$ (Fig. 6), though to a lesser degree than when the C-terminal structure is directly perturbed by mutagenesis (Poulsen 2010). The CAPOS mutation also causes an inward current in the

8

absence of extracellular K^+, which is not seen with the wild-type pump (Fig. 6A). The Na,K-ATPase is known to carry an inward current of H^+ under certain conditions, but usually not when high Na^+ levels are present extracellularly (Li et al 2006). The pump contains a hemichannel towards the third ion binding site which is controlled by the C-terminus. Disturbing the C-terminal structure was previously reported to cause inward currents and accelerated Na^+ release by opening of a hemichannel towards the third ion binding site (Poulsen 2010).

To test if Glu818Lys does indeed cause opening of the C-terminal structure, we performed Molecular Dynamic (MD) simulations from the structure of a K^+-occluded pump (Shinoda 2009). In agreement with the electrophysiological data, we found that Glu818Lys causes an opening of the C-terminal pathway that allows rapid entry of water molecules towards the ion binding site (Fig7A), but also that the effect is less pronounced than for direct mutations of the C-terminus (Fig 7B). Thus, the CAPOS mutation compromises pump function by destabilizing the Na^+-occluded state.

DISCUSSION

The patients presented here share remarkably similar histories - sudden episodes of neurological decline and ataxia, precipitated by febrile illness, and followed by progressive visual and hearing loss. In most cases, hearing loss was not apparent immediately, but some considerable time, often years, after the febrile episodes. It is unknown whether hearing was reduced or worsened during febrile episodes as has been reported by patients with temperature-sensitive AN related to *OTOF* gene mutations. (Starr et al, 1998, Zhang et al, 2016). Our cases, together with others presenting less well-reported features, such as seizures, athetosis, choreoathetosis, dystonia, autistic features and mild learning disabilities, suggest that the phenotype partially overlaps other *ATP1A3*-related disorders (RDP and AHC). However, optic atrophy and hearing impairment appear confined to the CAPOS mutation (Demos et al 2014; Rosewich et al 2014; Heimer et al 2015; Potic et al 2015; Maas et al 2016).

We report 18 patients of whom 11 are females and 7 are males, and in all four cases with transmission to subsequent generations this occurred through a female (figure 2). However among the cases in the literature there are 11 females and 11 males (Demos et al 2014;

9

Rosewich et al 2014; Heimer et al 2015; Potic et al 2015; Maas et al 2016) and the transmission in familial cases was through females in 4 instances (Demos et al 2014; Heimer et al 2015; Potic et al 2015) and through males in two cases (Demos et al 2014; Potic et al 2015). The gender distribution and transmission to a second generation therefore seems to be without any particular pattern.

The location of the residue Glu818Lys suggests that it impacts the C-terminal structure, and our electrophysiological characterization and molecular dynamics simulations confirm that it has effects similar to what was previously observed when mutating the C-terminus: very low affinity for extracellular sodium and a high rate of sodium release from the third ion binding site (Fig. 6). However, other mutations that affect the C-terminal structure, e.g. p.Asp992Tyr, cause AHC and not CAPOS. Furthermore, a substitution analogous to that in CAPOS, located very close by, p.Glu815Lys, is a hotspot for AHC (Pangiotakaki et al 2015; Viollet et al 2015). The p.Glu815Lys mutation causes a severe form of AHC with early onset, and biochemical studies suggest that it abolishes pump functionality (Weigand et al 2014). In CAPOS, it seems unlikely that pure loss-of-function would explain the deaf-blindness; the retinal and spiral ganglion neurons must be particularly affected by this one mutation. We therefore suspect that p.Glu818Lys confers a gain-of-function and/or an altered interaction with proteins specific to the ganglion neurons that future studies will be required to determine. However, the extended symptom pattern found in the 18 patients here, including the various movement disorders and psychological symptoms, which overlap with symptoms observed in RDP and AHC patients, could well be directly due to the observed impaired pumping, which will impact all α3 expressing neurons.

We demonstrate that hearing impairment in patients with CAPOS is an auditory neuropathy and that the lesion lies downstream of OHC function. Indeed, the presence of OAEs in 13 of the 15 cases tested here suggests that OHC function is intact as corroborated by cochlear microphonic potentials in case 17, where electrocochleography was performed, and the observation that ABRs were pathological or absent in all CAPOS patients. In auditory neuropathy, synchronized activation of afferent SGNs by glutamate release at IHC ribbon synapses and/or propagation of spikes along the auditory pathway are impaired, resulting in poor or absent CAP and ABR and degraded speech perception and binaural hearing (Giraudet and Avan, 2012; Rance and Starr, 2015; Moser and Starr, 2016).

Therefore, patients with auditory neuropathy characteristically describe difficulty with hearing and understanding speech, especially in noisy environments (documented in CAPOS cases), difficulty localizing sound, and reduced music appreciation. Speech recognition and ABRs are typically more severely affected than would be expected on the basis of pure tone audiograms (see Fig. 3 and Fig. 4 and Supplementary Information Cases 15,16,17,18).

The α3 subunit of the Na^+/K^+-ATPase encoded by the *ATP1A3* gene, shows highest expression in neurons; in the auditory system, it is prominently expressed in SGNs in the inner ear of several rodent species (McGuirt and Schulte 1994; Erichsen et al 1996; McLean et al 2009), both in the cell bodies and afferent terminals of myelinated nerve fibers contacting IHCs and in unmyelinated medial efferent neurons contacting OHCs (McLean et al 2009). As these efferent fibers are responsible for suppression of OHC activity, the high levels of α3 may explain why OAEs in some patients with CAPOS were unusually large (Cases 3, 14 and 17; Fig. S1, S4 and 4B).

Auditory neuropathy is important to diagnose because hearing rehabilitation differs from that of other types of sensorineural hearing impairment. Conventional hearing aids primarily amplify sound, and typically do not help auditory neuropathy subjects where the sound amplification by OHCs is intact (Rance and Starr 2015); in auditory neuropathy, it is the neural sound encoding and propagation of information which are impaired (Giraudet and Avan 2012). Instead, cochlear implantation, which directly stimulates the neural pathways, can successfully treat some forms of auditory neuropathy depending on the site of the lesion (Harrison et al 2015). For example, patients with disorders of IHCs, their synapses or the myelinated dendrites of SGNs (such as those due to missense mutations in *OPA1*) often benefit from cochlear implantation because the site of pathology can be bypassed by electrical stimulation (Santarelli et al 2015). In contrast, in disorders affecting distal myelinated dendrites, SGN cell bodies, or their central axons, the outcome of cochlear implantation is variable and many patients do not benefit (Rance and Starr 2015; Giraudet and Avan 2012). Interestingly, two of the four CAPOS patients with cochlear implants (the two youngest recipients, cases 15 and 16) have markedly benefitted as judged by improved speech recognition (see Supplementary Information).

Clinically, auditory neuropathy is straightforward to diagnose if the history is suggestive, and if the correct tests are performed. Investigations may lead to the diagnosis of a known syndrome or non-syndromic auditory neuropathy, as in the case of *OTOF* mutations, which exert their effect at the IHC synapse, and which may be successfully helped by cochlear implantation (Rodriguez-Ballesteros et al 2003; Rouillon et al, 2006; Santarelli et al, 2015). In CAPOS patients, severe visual impairment due to progressive optic atrophy on top of the auditory neuropathy presents an additional challenge in establishing a satisfactory mode of communication, particularly in those who rely on vision for lip reading. For patient management and prognosis, auditory neuropathy is an important diagnosis to make.

MATERIALS AND METHODS

Electrophysiology

Plasmids encoding human α3 and β1 subunits of Na^+/K^+-ATPase were purchased from Origene (Origene, Rockville, MD, USA) and subcloned into the pXOON vector using *EcoRI* and *NotI* (Jespersen et al 2002)). p.Glu818Lys was constructed with the quick change lightning site directed mutagenesis kit according to the manufacturer's instructions (Agilent Technologies). Constructs were sequenced to verify successful mutagenesis. α3 contains mutations p.Gln116Arg and p.Asn127Asp to reduce ouabain resistance (Price and Lingrel 1988).

In preparation of mRNA transcription, the plasmids were linearized using *NheI*, purified using standard phenol/chloroform extraction, and mRNA was transcribed using the mMessage mMachine T7 Ultra Kit (Ambion, Life Technologies, Carlsbad, CA, USA) according to manufacturer's instructions.

Oocytes from *Xenopus laevis* were isolated and defolliculated. 50 nl of a mixture of α3 (10 ng) and β1 (5 ng) mRNA was injected into Stage V and VI oocytes. Oocytes were incubated at 11 °C for 3–8 days prior to electrophysiological analysis.

Measurements were performed with an OC-725C voltage-clamp apparatus (Warner Instruments Corp., Hamden, CT, USA) and a Digidata 1440A (Molecular Devices, Sunnyvale, CA, USA) using the two-electrode voltage-clamp technique using buffers with or without 10 mM ouabain and otherwise: 115 mM NaOH, 110 mM succinic acid, 10 mM Hepes, 5 mM $BaCl_2$, 1 mM $MgCl_2$, 0.5 mM $CaCl_2$, 1 μM ouabain, pH 7.4. Measurements

were performed in 200 ms voltage jumps in steps of 20 mV. Data was recorded with pClamp 10.4 (Molecular Devices) and analysed with Graph Pad Prism 7 (Graph Pad Software). Measurements in buffer containing 10 mM ouabain were subtracted from measurements without to yield Na^+/K^+-ATPase specific pre-steady-state currents, which were fitted with single exponentials to determine charge translocation and rate constants were determined by fitting single exponentials.

Molecular dynamics simulations

All-atom MD simulations were performed using a similar protocol as in our previous studies of wild-type Na^+/K^+-ATPase and its mutants in various conformational states (Kopec et al 2014; Han et al 2017; Hilbers et al 2016). Here, the crystal structure of Na^+/K^+-ATPase from shark renal gland with bound MgF_4^{2-} and K^+ (PDB ID: 2ZXE, a stable analog of the $E2*Pi*2K^+$ state was used as a starting point of the simulations (Shinoda et al 2009). The protein crystal structure, including bound potassium ions, was embedded in a fully hydrated 1-palmitoyl,2-oleoyl-sn-glycero-3-posphocholine (POPC). The MgF_4^{2-} molecule was manually deleted prior to the insertion. Glu818Lys (Glu828Lys in shark renal gland numbering) and other C-terminal point mutations (Arg940Pro and Arg1005Gln in shark renal gland numbering, and also YY-AA, where two final tyrosines of the α subunit were replaced by alanines) (Poulsen et al 2010) were introduced with Pymol (The PyMOL Molecular Graphics System, Version 1.7.4 Schrodinger, LLC).

System construction – The K^+ coordinating residues: Glu334, Glu786 and Asp815 were kept protonated, as previously reported (Yu et al 2011). Additionally, charged residues involved in binding of the third Na^+ ion in E1 conformations of the pump, Asp933 and Glu961, were also protonated, as previously suggested (Poulsen et al 2010). The remaining glutamates and aspartates were kept in their charged forms. The Na^+/K^+-ATPase was embedded in an equilibrated POPC membrane (376 lipid molecules) and surrounded with ~63000 water molecules. Electroneutrality was achieved by adding an adequate number of K^+ ions, randomly placed in the aqueous solution prior to simulations.

Patients

Details on the patients in this report were collated after the diagnosis of CAPOS was made; the genetic studies were based on clinical suspicion (apart from case 18), typically after several years' search for a diagnosis. Clinical and audiological data have been collected retrospectively (for details see Tables 1 and 2 and Supplementary Material) except for data

13

from case 17 at age 14 which was acquired in the process of preparing the manuscript. Details are outlined in Supplementary Material.

Briefly, families 1 and 2 are unrelated and of Swedish origin; families 3, 4 and 5 are unrelated and of Danish origin; family 6 is French; families 7, 8 and 9 are from the UK, one of South Asian origin, the other two, British Caucasian; family 10 is German (reported previously but without detailed audiological data (Rosewich et al, 2014) and in family 11 the affected child has Spanish and Italian parents. Families 1, 2, 3, and 4 are two generation families (Fig. 2); the remainder are simplex. The patients ranged from 8 to 59 years at diagnosis.

Audiological examinations

OAE in case 17 (Figure 4) was performed using ILOv6, Otodynamics according to manufacturer's instructions. The rejection level was 49.5 dB SPL. DPOAE stimuli were 65/55 dB and the frequency ratio was 1.22.

Calculation of Pure Tone Averages ($PTA_{0,5,1,2,4 \text{ kHz}}$) and classification of the degree of hearing impairment followed the European recommendations (Mazzoli M et al, 2003), where 20-40 dB HL is mild; 41-70 dB Hl is moderate; 71-95 dB HL is severe; and >95 dB Hl is profound hearing impairment

Cochlear Microphonic

Identification of cochlear microphonic potentials was achieved in cases 3, 7, 9, 11, 12, 15, 16 and 17. In case 17 this was by electrocochleography. In the other cases, the cochlear microphonic was identified using a click ABR following recommended practice (http://www.thebsa.org.uk/wp-content/uploads/2015/02/CM).

Electrocochleography

Transtympanic electrocochleography was performed for case 17, using the Navigator pro system under sedation. The examination was done in the room adjacent to the MRI scanner (no electric or sound shielding) where other clinical data have been obtained in the same sedation which was necessary in order to avoid involuntary movements. A disposable monopolar needle electrode (902-DMG75-TP, Natus) was placed on the promontory and sound applied at a rate of 9.8 Hz via a custom-built 1m long plastic tube from a TDH39 loudspeaker/P210 amplifier to avoid electric artifacts from the sound system to superimpose

14

onto cochlear microphonic potentials based on a sound delay of 3 ms. Filters settings were:high pass 10Hz, low pass 5000 Hz, 50 Hz notch filter. Electrocochleography was performed in case 12 with Interacoustics Eclipse EP equipment under general anaesthesia using insert earphones, stimuli/sec 11,3, low pass 3000 Hz, high pass none, polarity: alternating. The recording room was an ordinary hospital room e.g. not a Faraday's cage or an audiometric booth.

Speech tests

Case 7 underwent Dantale I speech perception test (Elberling et al, 1989). Resukts are shown in Supplementary Material.

Case 17 underwent Oldenburger sentence test (Brand and Wagener, 2017).

Case 18 underwent The Goettinger Speech Test (Chilla et al, 1976), which measures speech understanding in children between 3 to 4 and 5 to 6 years of age. This test utilises a list of words or picture cards that must be repeated and matched to the correct word. This test is not performed in noise.

Case 18 also underwent a test for language skills called TROG-D (test zur Überprüfe des Grammatikverständnisses) (Kampfhaus RW, 2005), which is a German adapted test assessing grammatical comprehension in children aged 3-10. The test measures the understanding of 18 different sentence constructions; each sentence construction is presented four times each using different test stimuli.

Ophthalmological examination

Electrophysiological examinations were performed in accordance with principles of the International Society for Clinical Electrophysiology of Vision (Odom et al 2016; Odom et al 2010). Optical coherence tomography (OCT) scanning to measure retinal nerve fiber thickness profile (RNFL) was performed using the Heidelberg Spectralis version 1.7.0.0 (Heidelberg Engineering, Heidelberg, Germany) using the inbuilt software for scanning the optic nerve head.

Sanger Sequencing

ATP1A3 was sequenced by bi-directional Sanger sequencing using standard methods. Primer sequences are available on request.

Ethical aspects.

This is a retrospective study performed in accordance with Helsinki declaration. All patients have given informed consent to publish. For case 18 the study has been approved by the Ethics Committee of the University of Würzburg (approval number: 46/15).

Competing interests: None declared.

REFERENCES

-Attwell D and Laughlin SB (2001) An Energy Budget for Signaling in the Grey Matter of the Brain. J Cereb Blood Flow Metab 21:1133-1145.

-Bench J, Kowal A, Bamford J (1979) The BKB (Bamford-Kowal-Bench) sentence lists for partially-hearing children. Br J Audiol 13(3): 108-112.

-Boothroyd A (1968). Developments in speech audiometry. Br J Audiol (Sound);2:3-10

-Brand T, Wagener KC (2017) Characteristics, advantages, and limits of matrix tests (article in German). HNO 65(3): 182-188

-Chilla R, Gabriel P, Kozielski P, Bänsch D, Kabus M (1976) Der Göttinger Speech Kindersprachverständnistest I. HNO 24:342-346.

-Clausen MV, Hilbers F, Poulsen H (2017) The Structure and Function of the Na,K-ATPase Isofroms in Health and Disease. Front Physiol 8:371

-Dard R, Mignot C, Durr A, Lesca G, Sanlaville D, Roze E, Mochel F (2015) Relapsing encephalopathy with cerebellar ataxia related to an ATP1A3 mutation. Dev Med Child Neurol 57: 1183-1186.

-Demos MK, van Karnebeek,CD, Ross CJ, Adam S, Shen,Y, Zhan SH, Shyr C, Horvath G, Suri M, Fryer A,Jones SJM, Friedman JM and the FORGE Canada Consortium . (2014) A novel recurrent mutation in ATP1A3 causes CAPOS syndrome. Orphanet J Rare Dis 9: 15.

-Erichsen S, Zuo J, Curtis L, Rarey K, Hultcrantz M (1996) Na,K-ATPase alpha- and beta-isoforms in the developing cochlea of the mouse. Hear Res 100: 143-149.

-Geering, K (2005) Function of FXYD proteins, regulators of Na, K-ATPase. J Bioenerg Biomembr 37: 387-392.

18

-Giraudet F and Avan P (2012) Auditory neuropathies: understanding their pathogenesis to illuminate intervention strategies. Curr Opin Neurol 25: 50-56.

-Han M, Kopec W, Solov'yov IA , Khandelia H (2017) Glutamate Water Gates in the Ion Binding Pocket of Na+ Bound Na+, K+-ATPase. Sci Rep 7: 39829.

-Harrison RV, Gordon KA, Papsin BC, Negandhi J, James AL (2015) Auditory neuropathy spectrum disorder (ANSD) and cochlear implantation. Int J Pediatr Otolaryngol 79: 1980-1987.

-Heimer G, Sadaka Y, Israelian L, Feiglin A, Ruggieri A, Marshall CR, Scherer SW, Ganelin-Cohen E, Marek-Yagel D, TzadokM, Nissenkorn A, Anikster Y, Minassian BA, Zeev BB (2015) CAOS-Episodic Cerebellar Ataxia, Areflexia, Optic Atrophy, and Sensorineural Hearing Loss: A Third Allelic Disorder of the ATP1A3 Gene. J Child Neurol. 30: 1749-1756.

-Heinzen EL, Arzimanoglou A, Brashear A, Clapcote SJ, Gurrieri F, Goldstein DB, Jóhannesson SH, Mikati MA, Neville B, Nicole S, Ozelius LJ, Poulsen H, Schyns T, Sweadner KJ, van den Maagdenberg A, Vilsen B, and the ATP1A3 Working Group (2014). Distinct neurological disorders with ATP1A3 mutations. Lancet Neurol13(5): 503-514.

-Hilbers F, Kopec W, Isaksen TJ, Holm TH, Lykke-Hartmann K, Nissen P, Khandelia H, Poulsen H (2016) Tuning of the Na,K-ATPase by the beta subunit. Sci Rep 6 20442.

-Holmgren,M, Wagg J, Bezanilla F, Rakowski RF, De Weer P,Gadsby DC (2000) Three distinct and sequential steps in the release of sodium ions by the Na+/K+-ATPase. Nature 403: 898-901.

-Jespersen T, Grunnet M, Angelo K, Klaerke DA, Olesen SP (2002) Dual-function vector for protein expression in both mammalian cells and Xenopus laevis oocytes. BioTechniques 32: 536-538, and 540.

-Kampfhaus RW (ed.) (2005) Clinical Assessment of Child and Adolescent Intelligence, Springer, 2nd edition New York, NY,USA (ISBN-10:0-387-26299-7 and ISBN-13:978-0387262994)

-Kemp DT (1978) Stimulated acoustic emissions from within the human auditory system. J Acoust Am 64:1386-1391

19

-Kopec W, Loubet B, Poulsen H, Khandelia H (2014) Molecular mechanism of Na(+),K(+)-ATPase malfunction in mutations characteristic of adrenal hypertension. Biochemistry 53: 746-754.

-Li C, Geering K, Horisberger J-D (2006) The Third Sodium Binding Site of Na,K-ATPase Is Functionally Linked to Acidic pH-Activated Inward Current. J Membrane Biol 213:1-9.

-Maas RP, Schieving JH, Schouten M, Kamsteeg EJ and van de Warrenburg BP (2016) The Genetic Homogeneity of CAPOS Syndrome: Four New Patients With the c.2452G>A (p.Glu818Lys) Mutation in the ATP1A3 Gene. Pediatr Neurol 59: 71-75.e71.

-Mazzoli M, van Camp G, Nnewton V, Giarbini N, Declau F, Parving A (2003). Recommendations for the description of genetic and audiological data for families with nonsyndromic hereditary hearing impairment. Audiol Med 1: 148-150.

-McLean WJ, Smith KA, Glowatzki E, Pyott SJ (2009) Distribution of the Na,K-ATPase alpha subunit in the rat spiral ganglion and organ of corti. J Assoc Res Otolaryngol 10: 37-49.

-McGuirt JP and Schulte BA (1994) Distribution of immunoreactive alpha- and beta-subunit isoforms of Na,K-ATPase in the gerbil inner ear. JHistochemand Cytochem, 42 843-853

-Morth JP, Pedersen BP, Toustrup-Jensen MS, Sørensen TL-M, Petersen J, Andersen JP, Vilsen B, Nissen P (2017) Crystal structure of the sodium-potassium pump. Nature 450:doi:10.1038/nature06419.

-Moser T and Starr A (2016) Auditory neuropathy--neural and synaptic mechanisms. Nat Rev Neurol 12: 135-149.

-Nicolaides P, Appleton RE and Fryer A (1996) Cerebellar ataxia, areflexia, pes cavus, optic atrophy, and sensorineural hearing loss (CAPOS): a new syndrome 33: 419-421.

-Odom JV, Bach M, Brigell M, Holder GE, McCulloch DL, Mizota A, Tormene AP (2016) ISCEV standard for clinical visual evoked potentials: (2016 update). Doc Ophthalmol 133: 1-9.

-Odom JV, Bach M, Brigell M, Hoder,GE, McCulloch DL, Tormene,AP, Vaegan. (2010) ISCEV standard for clinical visual evoked potentials (2009 update). Doc Ophthalmol 120: 111-119.

20

-Panagiotakaki E, Grandis ED, Stagnaro M, Heinzenb EL, Fons C, Sisodiya S, de Vries B, Goubau C, Weckhuysen S, Kemlink D, Scheffer I, Lesca G, Rabilloud M, Klich A, Ramirez-Camacho A, Ulate-Campos A, Campistol J, Gianotta M, Moutard M-L, Doummar D, Hubsch-Bonneaud C, Jaffer F, Cross H, Gurrieri F, Tiziano D, Nevsimalova S, Neville B, van den Maagdenberg AMJM, Mikati M, Goldstein DB, Vavassori R, Arzimanoglou A, The Italian IBAHC Consortium, The French AHC consortium and the International AHC Consortium. (2015) Clinical profile of patients with ATP1A3 mutations in Alternating Hemiplegia of Childhood- a study of 155 patients. Orphanet J Rare Dis 10:123.

-Potic A, Nmezi B, Padiath QS (2015) CAPOS syndrome and hemiplegic migraine in a novel pedigree with the specific ATP1A3 mutation. J Neurol Sci 358**:** 453-456.

-Poulsen H, Khandelia H, Morth JP, Bublitz M., Mouritsen OG, Egebjerg J, Nissen P (2010) Neurological disease mutations compromise a C-terminal ion pathway in the Na(+)/K(+)-ATPase. Nature 467: 99-102.

-Price EM and Lingrel JB (1988) Structure-function relationships in the Na,K-ATPase alpha subunit: site-directed mutagenesis of glutamine-111 to arginine and asparagine-122 to aspartic acid generates a ouabain-resistant enzyme. Biochemistry 27 8400-8408.

-Rance G and Starr A (2015) Pathophysiological mechanisms and functional hearing consequences of auditory neuropathy. Brain : a journal of neurology 138: 3141-3158.

-Rodriguez-Ballesteros M, del Castillo F., Martin Y, Moreno-Pelayo MA., Morera C, Prieto F, Marco J, Morant A, Gallo-Teran J, Morales-Angulo C, Navas C, Trinidad G, Cruz Tapia M, Moreno F, del Castillo I. (2003) Auditory neuropathy in patients carrying mutations in the otoferlin gene (OTOF). Hum Mutat 22: 451-456.

-Rosewich H, Weise D, Ohlenbusch A, Gartner J , Brockmann K (2014) Phenotypic overlap of alternating hemiplegia of childhood and CAPOS syndrome. Neurology 83**:** 861-863.

-Rouillon I, Marcolla A, Roux I, Marlin S, Feldmann D, Couderc R, Jonard L, Petit C, Denoyelle F, Garabédian EN, Loundon N. Results of cochlear implantation in two children with mutations in the *OTOF* (2006). Int J Pediatr Otorhinolaryngol 70 (4): 689-696.

-Santarelli R, Rossi R, Scimemi P, Cama E, Valentino ML, La Morgia C, Caporali L, Liguori R, Magnavita V, Monteleone A, Biscaro A, Arslan E, Carelli V (2015) OPA1-related auditory neuropathy: site of lesion and outcome of cochlear implantation. Brain 138: 563-576.

-Schuth O, McLean WJ, Eatock RA, Pyott SJ (2014). Distribution of Na,K-ATPase αsubunits in rat vestibular sensory epithelia. J Assoc Res Otolaryngol 15: 739-754

-Shinoda T, Ogawa,H, Cornelius F, Toyoshima C (2009) Crystal structure of the sodium-potassium pump at 2.4 A resolution. Nature 459: 446-450.

-Starr A, Picton TW, Sininger Y, Hood LJ, Berlin CI (1996) Auditory neuropathy. Brain 119 (Pt 3): 741-753.

-Starr A, Siniger YS, Winter M, Derebery MJ, Oba S, Michalewski HJ (1998) Transient deafness due to temperature-sensitive auditory neuropathy. Ear Hear 19 (3): 169-179.

-Sweney MT, Newcomb TM, Swoboda KJ (2015) The expanding spectrum of neurological phenotypes in children with ATP1A3 mutations, Alternating Hemiplegia of Childhood, Rapid-onset Dystonia-Parkinsonism, CAPOS and beyond. Pediatr. Neurol, 52: 56-64.

-Viollet L, Glusman G, Murphy KJ, Newcomb TM, Reyna SP, Sweney M, Nelson B, Andermann F, Andermann E, Acsadi G, Barbano RL, Brown C, Brunkow ME, Chugani HT, Cheyette SR, Collins A, DeBrosse SD, Galas D, Friedman J, Hood L, Huff C, Jorde LB, King MD, LaSalle B, Leventer RJ, Leweit AJ, Massart MB, Mérida II, MR, Ptáček LJ, Roach JC, Rust RS, Renault F, Sanger TD, de Menezes MAS, Tennyson R, Uldall P, Zhang Y, Zupanc M, Xin W, Silver K, Swoboda KJ (2015). Alternating Hemiplegia of Childhood: Retrospective Genetic Study and Genotype-Phenotype Correlations in 187 Subjects from the US AHCF Registry. PLoS One May 21; 10(5):e0127045.doi:10.1371/journal.pone.0127045. Erratum in PLoS One 2015;10(8):e0137370.

-Watts AG, Sanchez-Watts G, Emanuel JR, Levenson R. (1991) Cell-specific expression of mRNAs encoding Na^+,K^+-ATPase α- and β-subunit isoforms within the rat central nervous system. Proc natl Acad Sci USA 88: 7425-7429.

-Vedovato N, Gadsby DC (2010) The two C-terminal tyrosines stabilize occluded Na/K pump conformations containing Na or K ions. J Gen Physiol 136: 63-82

-Weigand KM, Messchaert M, Swarts HG, Russel FG, Koenderink JB (2014) Alternating Hemiplegia of Childhood mutations have a differential effect on Na(+),K(+)-ATPase activity and ouabain binding. Biochim Biophys Acta 1842: 1010-1016.

-Yaragatupalli S, Olivera JF, Gatto C, Artigas P (2009) Altered Na^+ transport after an intracellular - α-subunit deletion reveals strict external sequential release of Na^+ from the Na/K pump. Proc Natl Acad Sci USA 106(36): 15507-15512.

-Yu H, Ratheal IM, Artigas P,Roux B (2011) Protonation of key acidic residues is critical for the K(+)-selectivity of the Na/K pump. Nat Struct Mol Biol 18: 1159-1163.

Zhang Q, Lan l, Shi W, Yu L, Xie L, Xiong F, Zhao C, Li N, Yin Z, Zong L, Guan J, Wang D, Sun W, Wang Q (2016). Temperature sensitive auditory neuropathy. Hear Res 335:53-63-

23

Figure legends

Fig. 1. **Schematic of the catalytic cycle of the Na,K-ATPase.** The forward reaction of the pump is clock-wise. The membrane is indicated by horizontal lines with the extracellular compartment denoted 'ex' and the cytoplasm denoted 'in'. In the so-called E1 state, the enzyme has high affinity for sodium, and in the E2 state it has high affinity for potassium. During the cycle, the enzyme acts as both substrate, kinase and phosphatase, and the phosphorylated states of the pump are denoted with a P (E1P and E2P). Starting in the top left corner, the pump has three Na^+ (blue spheres) occluded in the E1P state that are released extracellularly when the pump opens to the outside in the E2P state. The open pump will bind two K^+ (red spheres) and dephosporylate to the E2 state where the K^+ are occluded . Opening of the pump on the intracellular side and transition to the E1 state allows release of K^+ and binding of Na^+. With phosphorylation of the pump, the Na^+ are then occluded in the E1P state. The P in the E1P and E2P states signifies that the pump is phosphorylated by the ATP that provides the energy for the transport. A full circle depends on intracellular Na^+ and ATP and extracellular K^+. The grey square indicates that in the absence of extracellular K^+ and intracellular ADP, the pump is restricted to transitions between E1P and E2P, i.e. extracellular release and binding of Na^+.

Fig. 2. **Pedigrees of four of the families investigated in the study (a-d)**. All the families (families 1,2,3,4) show segregation of the *ATP1A3* mutation c.2452G>A;p.Glu818Lys with the disease. Probands are indicated by arrows. The *ATP1A3* molecular result is indicated below each individual who provided DNA. N = normal allele. Vertical line through a symbol means age -related hearing impairment. A diagonal line through an individual indicates that the person is deceased and a double-line between two parents indicates consanguinity.

Fig. 3. **Audiograms from cases 1, 5, 6, and 7 .** Case 1 shows progressive hearing loss in the right ear. Cases 5, 6, and 7 demonstrate that low frequencies are predominantly affected and that the hearing loss is symmetrical.

Fig. 4. **Clinical data from case 17**. A, Audiograms at 12 years (pink/light blue) and 14 years (red/blue) of age. B, TEOAE and DPOAE with high amplitudes. C, ABR to rarefaction (upper traces) and alternating (lower traces) click stimuli are absent (example left ear). A normal ABR is shown below in red with expected waveforms indicated. D, recording technique for transtympanic electrocochleography (ECochG): a needle is placed on the promontory, the bone covering the

cochlea. The reference electrode (not shown) is on the contralateral mastoid. Sound stimuli are administered via a loudspeaker. E, summating potential/compound action potential complexes (arrows) to click stimulation in the patient (left ear; blue) have a very low amplitude, but the peak latency is comparable to that of a normal-hearing proband (representative example in red, bottom). Right: In response to 500 Hz tone burst stimulation, cochlear microphonic potentials were present. Black lines in E indicate the time of stimulus onset. Data were acquired at age 14.

Note the scale bar difference between the patient data and the example of normal ECochG recording and the difference in the shape of the click response.

Fig. 5. **Structural context of p.Glu818.** A, The tripartite pump is shown with the α subunit in grey, the β subunit in blue, and the γ subunit in green. The membrane is indicated with horizontal lines, the cytoplasm is below. The two occluded potassium ions are visible as red spheres in the middle of the membrane. P.Glu818 (yellow sticks) is in the transmembrane part of the pump on the cytoplasmic side, close to the C-terminus (magenta sticks). B, A close-up of the structure around p.Glu818, viewed from the cytoplasmic side. The p.Glu818 carboxyl is less than 3Å from the backbone amide of Arg930, which coordinates the C-terminus. Figures made with Pymol using pdb 2ZXE.

Fig. 6. **The CAPOS mutation affects the E1P-E2P equilibrium.** A, The ouabain-sensitive pre-steady-state currents of wild-type and p.Glu818Lys human Na^+/K^+-ATPase α3, co-expressed with β1 in *Xenopus laevis* oocytes, shows binding and release of extracellular sodium. B, Fitting of single exponentials to pre-steady-state currents as shown in C allows the charge Q moved to be determined (top). The midpoint potential V_{50} for the wild-type is -72 mV +/- 39 mV, and for Glu818Lys it is -202 mV +/- 40 mV. The rates (bottom) are also determined from the pre-steady-state currents, and the rates for the mutant are higher than for the wild-type.

Fig. 7. **MD simulations of the effect of the CAPOS mutation on the C-terminal structure.** A, The degree of hydration of residue p.Asp933 at the third binding site is evaluated. The radial distribution functions g(r) between p.Asp933 and water molecules shows a peak for r < 5Å if the residue is hydrated. No peak is observed for the wild-type, but a clear peak is seen for p.Glu818Lys. Similarly, other mutations affecting the structure terminus (p.Arg940Pro, p.Arg1005Gln and YY-AA) also cause hydration of p.Asp933. B, The radius of the bottleneck of the pathway was determined. In the wild-type, the radius is narrow, and the channel is closed, while p.Glu818Lys

causes an opening of the channel. Other mutations directly affecting the C-terminus cause even larger openings.

Legends for Supplementary figures S1-S7

Fig. S1. Representative sequence chromatograms for the *ATP1A3* missense mutation c.2452G>A; p.Glu818Lys compared to a normal control. The arrow indicates the nucleotide change of the heterozygous missense mutation. Nomenclature of mutation refers to the *ATP1A3* RefSeq NM_152296.4, (Gene ID: NG_008015.1) with nucleotide number +1 being A of the start codon ATG.

Fig. S2. A, Preserved OAEs at age 13 in case 3, with noticeable high amplitudes. B, ABR (calibrated in dB peSPL) from left and right ear in case 3 without reproducible responses

Fig. S3. Case 12 at age 19 years. A Air conduction thresholds for right (red symbols) and left (blue symbols) ear. B. ABR with click stimulus in rarefaction and condensation mode, right and left ear. Phase-reversed cochlear microphonics at 80 dB nHL and higher intensities in combination with no stimulus artefact. C. Transtympanic electrocochleography with alternating click (right ear). A large summation potential is seen with threshold at 50 dB nHL pointing to preserved inner hair cell function.

Fig. S4. Case 14

A, Pure tone audiograms at age 29 years (pale lines) and at 32 years (dark lines) showing some progression in the right ear (red) and possibly in the left ear (blue). B, TEOAE and DPOAE are present in both ears. TEOAE Stimulus 83.7 and 85.8 dBpe, reject level = 48.0dBspl; DPOAE Stimulus = 70/70 dB; 8 pts/octave; F2/F1 – 1.22; reject level = 49.5 dBspl, Otodyamics Ltd ILOv6 C, Click ABR shows no repeatable response at 100 dB nHL in either ear.

Fig. S5. Case 15

A, Pure tone audiogram at age 11 years showing moderate hearing loss. B, TEOAE and DPOAE are present. TEOAE Stimulus 85.8 and 86.9 dBpe, reject level = 49.5 dBspl; DPOAE, Stimulus = 65/55 dB; 3 pts/octave; F2/F1 – 1.22; reject level = 49.5 dBspl, Otodyamics Ltd ILOv6 C, Tone pip ABR shows no repeatable response at 80dBnHL at 4kHz. D, Click ABR showing cochlear microphonics are present in both ears, more marked on the right. Note that primary low frequencies are affected.

Fig. S6. Case 16

A, Pure tone audiograms at age 8 years (pale lines) and 9 years (dark lines) showing severe low and high frequency hearing impairment on the right and profound low and moderate hearing loss on the left ear. There has been progression at 500 Hz in the left ear. B, TEOAE and DPOAE are present in both ears at age 7 years. TEOAE Stimulus 83.7 and 83.7 dBpe, reject level = 54.0 and 50.9 dBspl; DPOAE Stimulus = 65/55 dB; 3 pts/octave; F2/F1 − 1.22; reject level = 49.5 dBspl, Otodyamics Ltd ILOv6 C, Click ABR shows no repeatable response at 90dB nHL in either ear. D, Click ABR shows cochlear microphonics are present in both ears.

Fig. S7. Optical Coherence Tomography (OCT) measuring the retinal nerve fiber thickness profile (RNFL) from case13. A) Retinal nerve fiber (RNFL) thickness profile (black curve) in case 13 at age 13 years shows a reduced RNFL thickness in all quadrants, temporal (TMP), superior (SUP), inferior (INF) and nasal (NAS) sides, in both eyes. OD, right eye; OS, left eye. The green area defines the 5th to 95th (normal thickness), the yellow area the 1st to 5th (border-line thickness) and the red area below the first percentiles (abnormal thickness). Color scale of the thickness profile is indicated in the color bar at the bottom of the figure.

On the right, RNFL thickness in individual sectors and clock hours demonstrates decreased RNFL thickness in the superior (S), inferior (I), nasal (N) and temporal (T) quadrants of right and left eyes. RNFL measurements in corresponding quadrants is noted in μm. The table represents key parameters of optic nerve head and RNFL analysis. There is severe decreased average RNFL thickness with an average RNFL thickness of 45.22μm in the right eye and 47.22μm in the left eye. B) Eye fundus picture of affected case13 shows pale, almost white optic nerve of the left eye at age 26 years. In unaffected people the optic nerve appears pink.

Table 1 Cases 1-6

Subject	Case 1	Case 2	Case 3	Case 4	Case 5	Case 6
Family	family 1	family 1	family 1	family 1	family 2	family 2
Nationality	Swedish	Swedish	Swedish	Swedish	Swedish	Swedish
Sex and age (2016)	female 52y	male 31y	male 27y	female 17y	female 51y	female 30y
Age of onset of neurological dysfunction	10m	1y	6y	3y	1y	2y
Number of episodes	5	4	2	2	4	1
Abnormal eye movements	Yes	Yes at 32 m	NI	NI	Yes, nystagmus 34m	Yes, nystagmus 2y
Age at last episode	23y	5y	4y	16y		2y
Febrile trigger	Yes	Yes	Yes	Yes	Yes	Yes
Seizures	No	Yes at 20m	No	No	Yes	Yes
Optic atrophy	Yes	Yes at 34m	Yes at 6.5y	No at 5y	Yes at 22m	Yes at 34m
Visual acuity	0.13 at 38y	0.15/0.2 at 5.5y	0.5 at 3.5y	O.U 1.0 age 5y, myopia, otherwise normal at 7y & 11y	0.05/0.1 age 8y	0.3 at 34m; 0.3 at 13y
OCT	NI	NI	NI	NI	NI	NI
VEP	Abnormal at 23y	Abnormal at 3y	NI	NI	NI	Abnormal at 34m
Hearing Loss	Yes	Yes, moderate at 5y	Yes	Yes	Yes at 30m	Yes
Auditory Neuropathy	Yes	Yes	Yes	Yes	Yes	Yes
Cerebellar ataxia	Yes	Yes	Yes	Yes	Yes	Yes
Areflexia	Yes	Yes	Yes	Yes	Yes	Yes
Pes cavus	Yes	Yes	Yes	Yes at 3y	Yes at 3y	NI
Dystonia	Athetosis; wheel chair bound	Yes, from 1y	Choreoathetosis of trunk	NI	Athetosis; improved in pregnancy at 26y	Athetosis
Autistic features	No	Yes	No	Yes	No	No

Neuropathy	Axonal neuropathy	Axonal neuropathy	NCV normal at 13y	EMG and NCV at 5y normal	No	NI
CT/MRI scan	CT and MRI: normal at 23y	CT normal at 24m; MRI normal at 16y	CT normal; MRI thin brainstem, wide 4th ventricles at 13y	CT normal; MRI normal at 5y	CT normal at 16y	MRI at 13y: narrow cerebellar peduncles and pons

Cases 7-12

Subject	Case 7	Case 8	Case 9	Case 10	Case 11	Case 12
Family	family 3	family 3	family 4	family 4	family 4	family 5
Nationality	Danish	Danish	Danish	Danish	Danish	Danish
Sex and Current age (2016)	female 33y	female 60y	female 23y	female 26y	female 47y	male 22y
Age of onset of neurological dysfunction	8m	4y	20m	3y	4y	3m
Number of episodes	2	1	2	2	NI	3
Seizures	Yes at 5y	NI	Yes at 20m	NI	NI	Yes at 3y
Abnormal eye movements	Yes, nystagmus at 5y	NI	Yes, nystagmus at 3y	Yes	Yes	NI
Age at last episode	5y	NI	NI	13y	NI	7y
Febrile trigger	Yes	Yes	Yes	Yes	Yes	Yes
Optic atrophy	Yes at 16y	Yes at 43y	Yes at 4y	Yes at 13y; confirmed 25y	Yes from at 30y	Yes at 8y; confirmed at 21y
Visual acuity	0.3/0.4 at 27y; ERG normal at 27y	O.D.: 0.3, and O.S.: 0.4 at 43y; ERG normal at 43y	0.1/0.2 at 22y	0.9 OU at 10y; 0.125 at 25y	Extinguished color vision from at 30y; O.D:0.1; O.S:0.15 at 30y	Severe CVI, light perception
OCT	Abnormal at 32	NI	NI	NI	NI	Not possible due to spasticity
VEP	Abnormal at 27y	Abnormal at 43y	Abnormal at 22y	Severely abnormal at 25y	NI	Abnormal 21y
Hearing loss	Yes at 5y	Yes, progressive, profound at 57y	Yes,	Yes, progressive	Yes , severe at 30y	Yes, moderate HI at age 12y, no verbal language; normal hearing 6y
Auditory neuropathy	Yes	Yes	Yes	Yes	Yes at 42y	Yes - postsynaptic AN
Cerebellar ataxia	Yes	Balance problems	Yes	Yes	NI	Yes

Areflexia	Yes	Yes	Yes	Yes	NI	Yes
Pes cavus	No	NI	NI	NI	NI	NI
Dystonia	No	No	Athetoid movements at 20m; wheelchair bound	Severe dystonia at 12y: wheelchair bound; treated with baclofen pump, and botulinum toxin	NI	Dystonia 16m, ; baclofen pump (1997-2001); wheelchair bound
Autistic features	No	No	No	No	No	No
Neuropathy	NI	No	No	No	No	NI
CT/MRI scan	CT: normal at 5y MRI (33y):Atrophic cochlear nerve without IAC hypoplasia	ENG and NCV normal at 38y	CT normal at 20m, MRI normal at 15y	MRI normal at 24y	CT normal at 43y; MRI normal at 42y	MRI normal at 3y; at 6y central and cortical atrophy, normal basal ganglia; normal spectroscopy; CT temporal bone normal at 18y; MRI at age 19 y normal

Cases 13-18

Subject	Case 13	Case 14	Case 15	Case 16	Case 17	Case 18
Family	family 6	family 7	family 8	family 9	family 10*	family 11
Nationality	French	British	British	British Asian	German	Spanish/ Italian
Sex and Current age (2016)	male 30y	male 35y	female 13y	female 18y	male 13y	male 8y
Age of onset of neurological dysfunction	14m	22m	18m	18m	20m	Multiple
Number of episodes	2	2	3	4	Multiple	Multiple
Febrile trigger	Yes	Yes	Yes	Yes	Yes	No; from age 2 attacks of reduced physical activity, and confinement to bed
Age at last episode	20y	9y	10y	10y	6y	NA
Abnormal eye movements	No	Yes, pendular nystagmus	No	Yes, intermittent nystagmus	No	No
Seizures	NI	No	No	No	No	No
Optic atrophy	Yes at 4y	Yes	Yes mild at 12y	Yes	Yes at 12 y	Only auditory neuropathy 6y**
Visual acuity	VA decreased at 14y; VA:0.1 at 20y; normal color vision & ERG 20y	Reduced from 20y	0.22/0.16 at 12y; ERG normal age 10y	0.7/0.8 at 11y 0.94/1.02 at 13y	0.3 at 12y	
OCT	Thinned retinal nerve fiber layer at 26y	NI	Thinning of nerve fibre layer at 10y	NI?	NI	NI
VEP	Abnormal	Abnormal at 32y	Abnormal at 10y	Abnormal at 7y,10y	Abnormal at 12y	NI
Hearing Loss	Yes at 4y; fluctuating, progressive	Yes, moderate to severe (upsloping); progressive	Yes; low frequency. Progressive	Yes at 5y, low and mid-frequency progressive	Yes at 6y, low frequency	NI

Feature						
Auditory Neuropathy	Yes; moderate to severe (flat) on R	Yes; normal to profound in 5y	Yes	Yes at 5y	Yes	Yes
Cerebellar ataxia	Yes at 14 m	Yes	Yes, very mild	Yes	Yes	Unsteady gait and clumsy
Areflexia	NI	Yes	Yes	Yes	Yes	Yes
Pes cavus	NI	Yes	No	No	No initially, but has high arches	No
Dystonia	NI	No	No	No	No, choreiform at times; titubation	Yes, mild
Autistic features	No	No	Withdrawn	No	Behaviour problems initially	No
Neuropathy	NI	NI	Normal EMG and NCV at 9y	Normal NCV at 3y, 8y, 11y	No	No
CT/MRI scan	MRI normal at 15y	MRI normal at 22y	MRI normal at 10y	MRI normal at 3y, 7y, 11y	MRI normal at 2y; Proton MRS normal lactate	MRI normal at 6y

Legend for Table 1

Summary of clinical features. ** see Supplementary information for details

CVI = central visual impairment (cause of visual problems are of central nervous origin); ERG = electroretinogram; IAC = internal auditory canal;

L = left; m = months; NA = not applicable; NI = no information; O.D = oculus dexter (right); O.S = oculus sinister (left); O.U = oculi utrisque

(both eyes); R = right; VA = visual acuity; y = years

* (Rosewich H et al, 2014)

Table

Table 2. Detailed Audiological features

Patient	ABRs/PTA$_{0.5-4}$ kHz R/L dB (age)*	OAEs	Speech recognition	Diagnosis of HI (age)	Diagnosis of CAPOS	Cochlear micro-phonics	Vestibular dysfunction	Progression of HI	Treatment
case 1 family 1	Abnormal 64/74(7y)	Absent (at 38y)	NI	7y	51y	NI	Yes (38y)	Yes Moderate→severe	HA
case 2 family 1	Abnormal 63/69 (14y)	Present (9y)	NI	5y	30y	NI	Yes (16y)	NI Moderate	HA
case 3 family 1	Abnormal 40/34 (5y)	Present (13y)-high amplitude	NI	4y-low frequencies	26y	Yes	NI	Yes Mild	HA
case 4 family 1	Abnormal 38/29 (11y)	Present (10y)	NI	11y-low frequencies	16y	NI	NI	No Mild	HA 10y
case 5 family 2	Abnormal 86/93 (4y)	NI	Poor	30m-low frequencies	50y	NI	Severe 7y	Yes Severe→profound	HA
case 6 family 2	Abnormal 46/31 (10y)	Present (10y)	NI	3y	29y	NI	Weak caloric response at 10y	Yes Mild→Severe	HA
case 7 family 3	Abnormal 55/65 (25y)	Present	Poor*	5y	32y	Yes	NI	Yes Moderate	HA*
case 8 family 3	Abnormal 75/79 (25y)	NI	Poor	4y	59y	NI	NI	Yes Severe→Profound	HA
case 9 family 4	Abnormal 56/57 (17y)	Pass/refer (18y)	Poor formal testing not done	3.5y	22y	Yes	NI	Yes Moderate	HA; CI 19y

case 10 family 4	Abnormal 45/58 (21y)	Present (25y)	Poor formal testing not done	10y	25y	NI	NI	Yes Moderate	HA 10y
case 11 family 4	Abnormal 95/99 (33y)	NI	Poor	4y	46y	Yes	NI	Yes Severe	HA 4y; CI 43y
case 12 family 5	Abnormal 53/56 (18y)	Present (19y)	Poor formal testing not done	12y	21y	Yes	NI	Yes Moderate	HA 6y; CI considered*
case 13 family 6	Abnormal 88/93 (26y)	Absent at 26y	Poor	10y	29y	NI	Yes at 26y	Yes Severe	HA 6y
case 14 family 7	Abnormal 54/49 (29y)	High amplitude	Poor hearing in noise	10y	34y	NI	NI	Yes Moderate→ Moderate/ severe	HA
case 15 family 8	Abnormal 53/48 (12y)	Present	Poor	5y	12y	Yes	No, 10y	Yes Moderate	HA 5y; CI 12y
case 16 family 9	Abnormal 34/34 (8y)	Present*	Poor	5y	17y	Yes	Yes	Yes Mild→mild/ moderate	HA; CI 10y, 16y
case 17 family 10	Abnormal 27/29 (12y)	High amplitude	Poor hearing in noise	11y	12y	Yes	NI	yes Mild Mild /moderate	-
case 18 family 11	NI 24/18 (6,6y)	Present (6y)	Poor	6y-low frequencies	8y	NI	NI	No Mild	HA

NI = no information

HA = Hearing Aid

CI= cochlear implant ; *see Supplementary material. $PTA_{0.5-4\ kHz}$ R/L dB means averaged PTA in dB HL of right-R, and left-L ear, respectively.

classification of degree of hearing impairment according to Mazzoli M et al (2003)
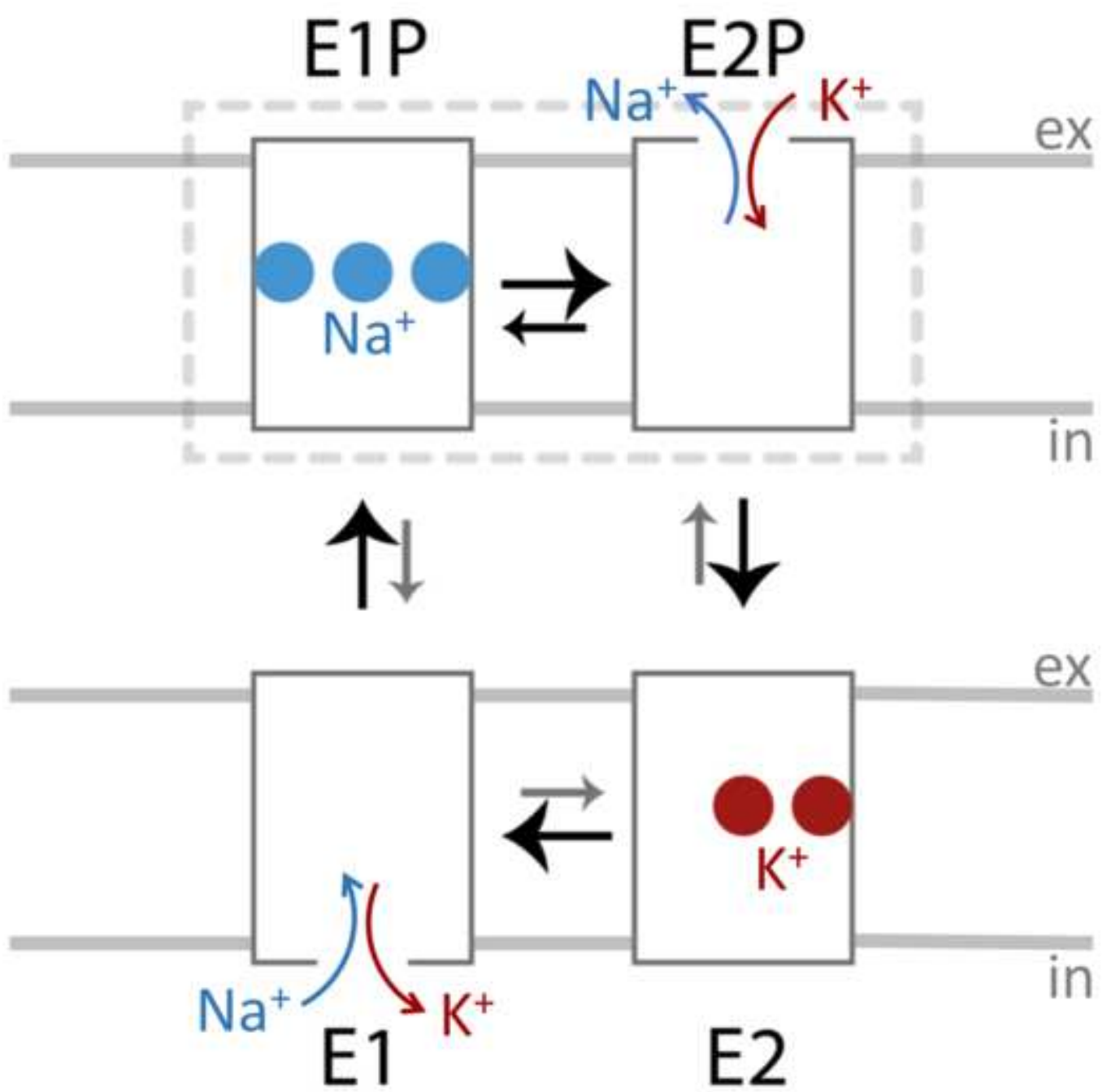
A. Family 1
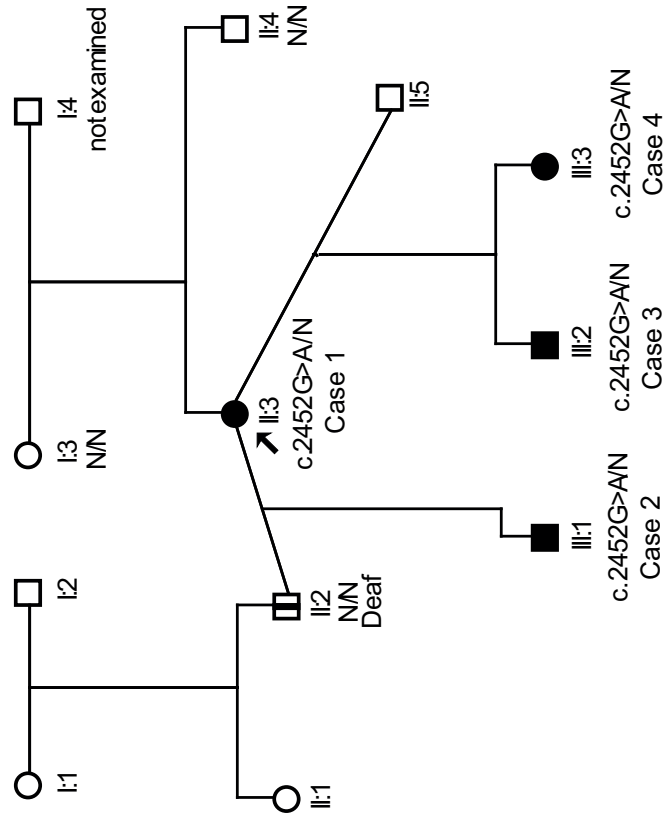
B. Family 2

C. Family 3

D. Family 4

Fam 1, case 1
7 and 26 years

Fam 2, case 5
3.5 and 37 years

Fam 2, case 6
9 years

Fam 3, case 7
25 years

Figure

A

β

α

Glu818

FXYD

B

Arg930

C-terminus

2.57Å

Glu818

Figure

Figure
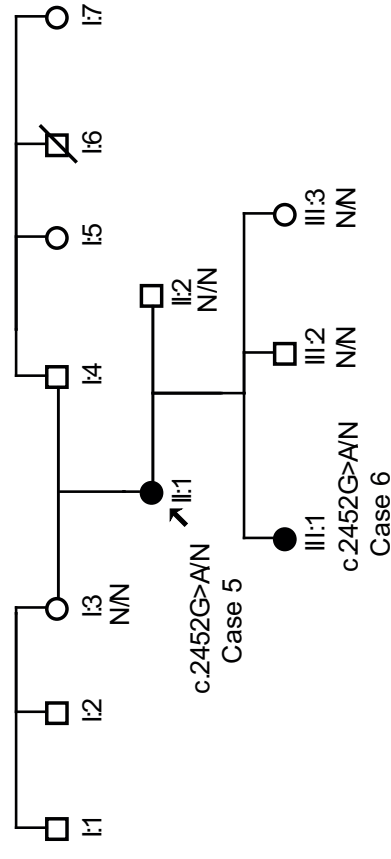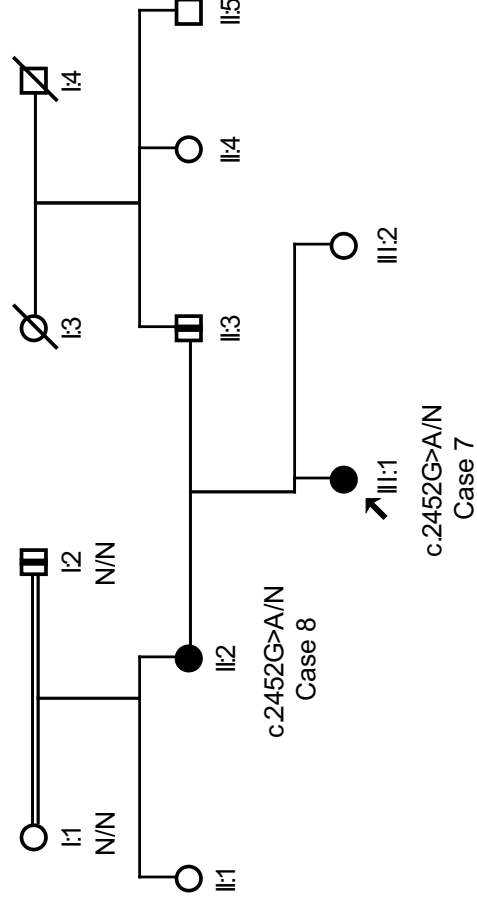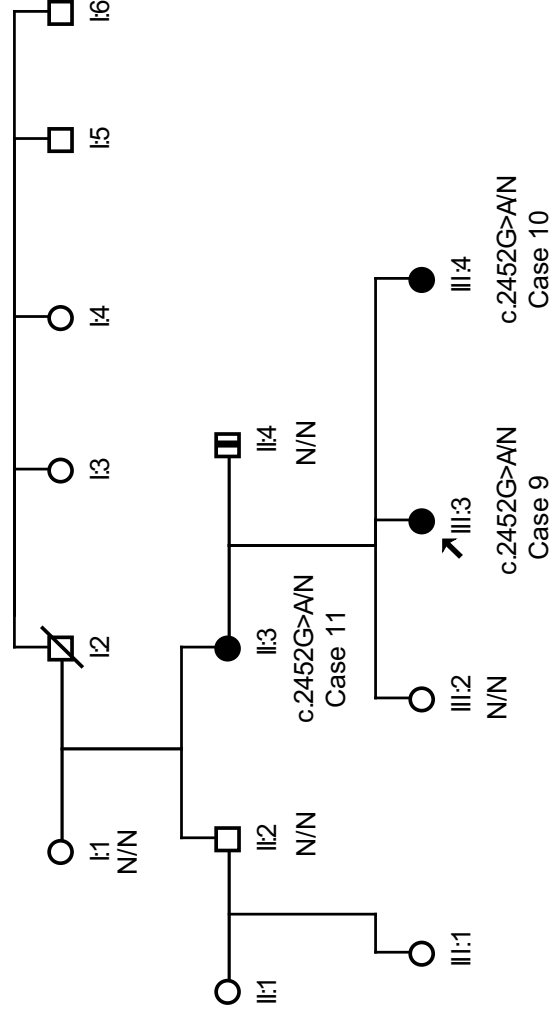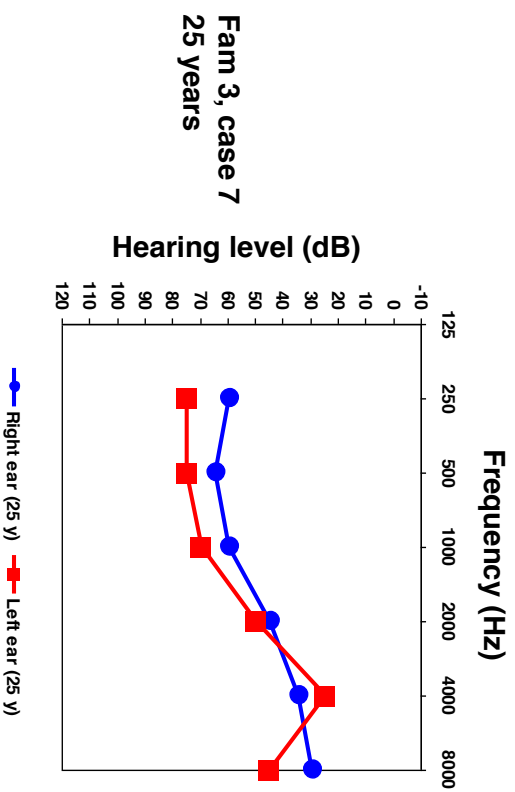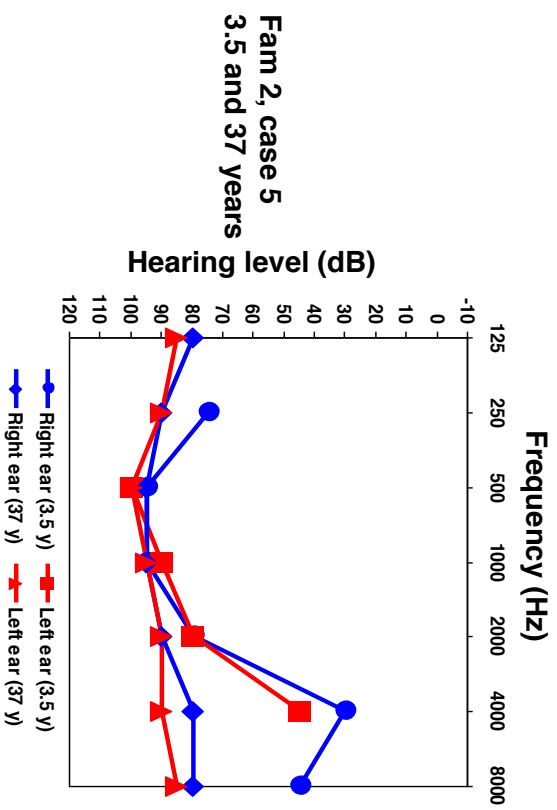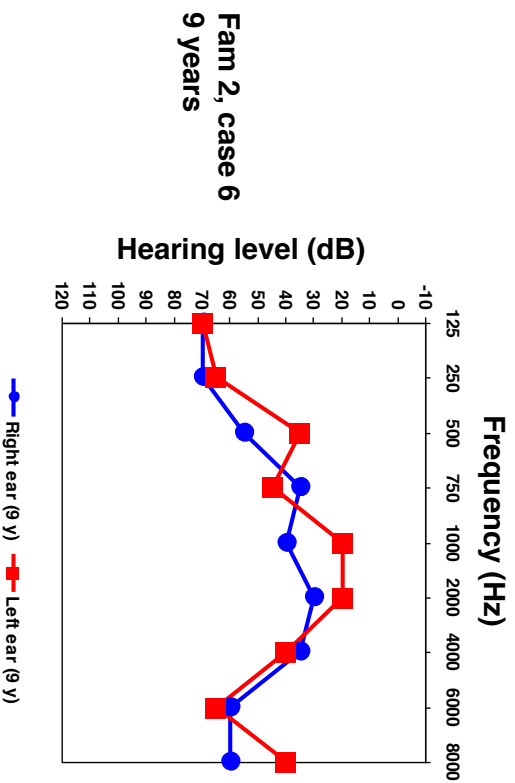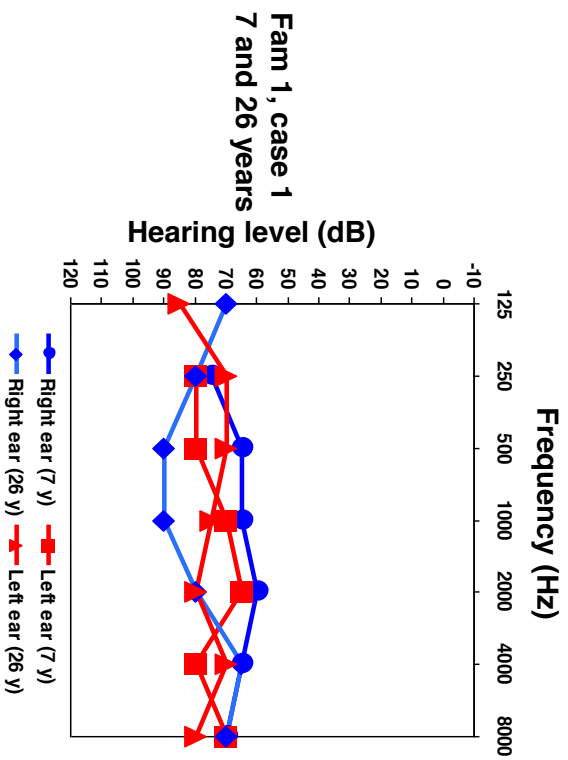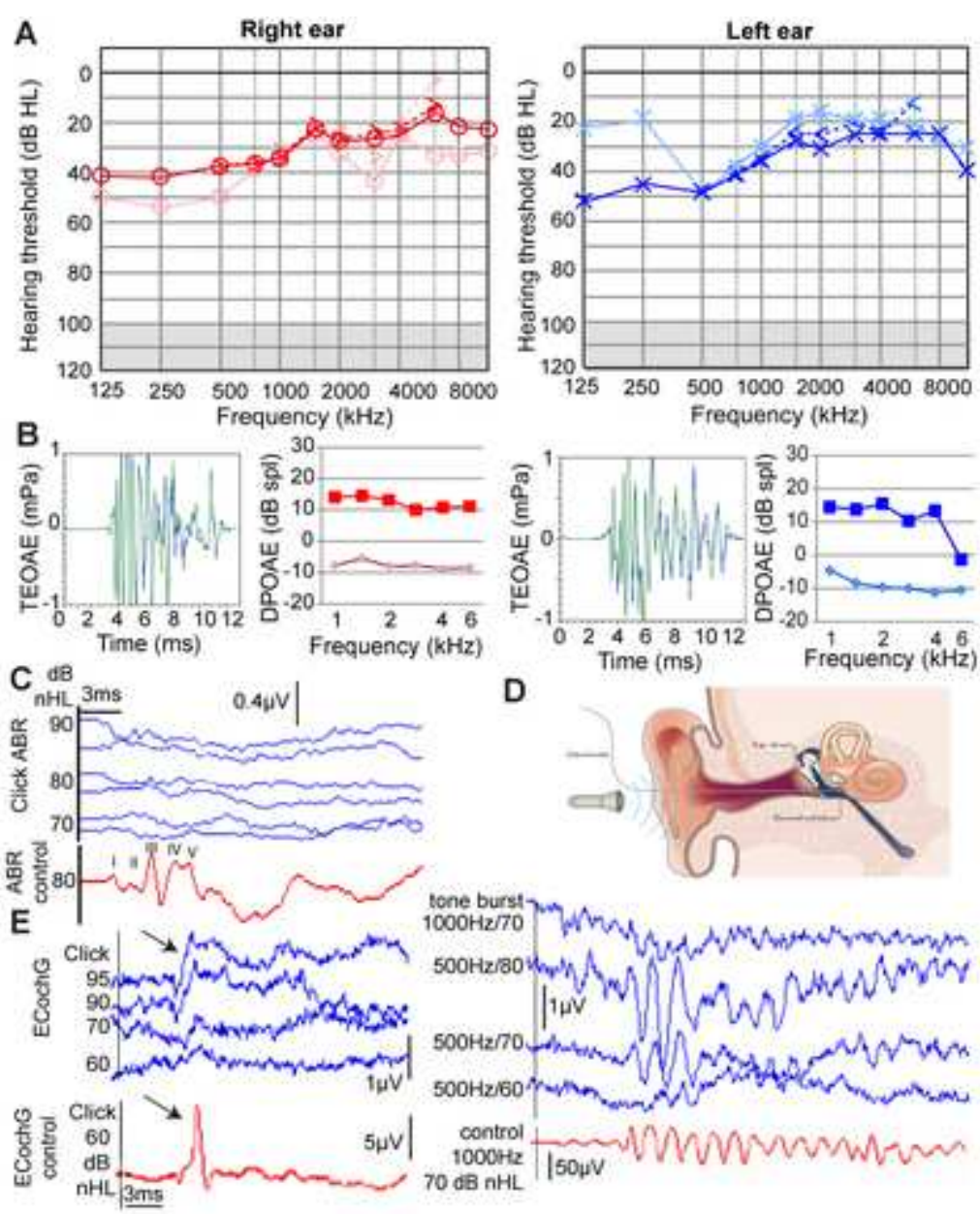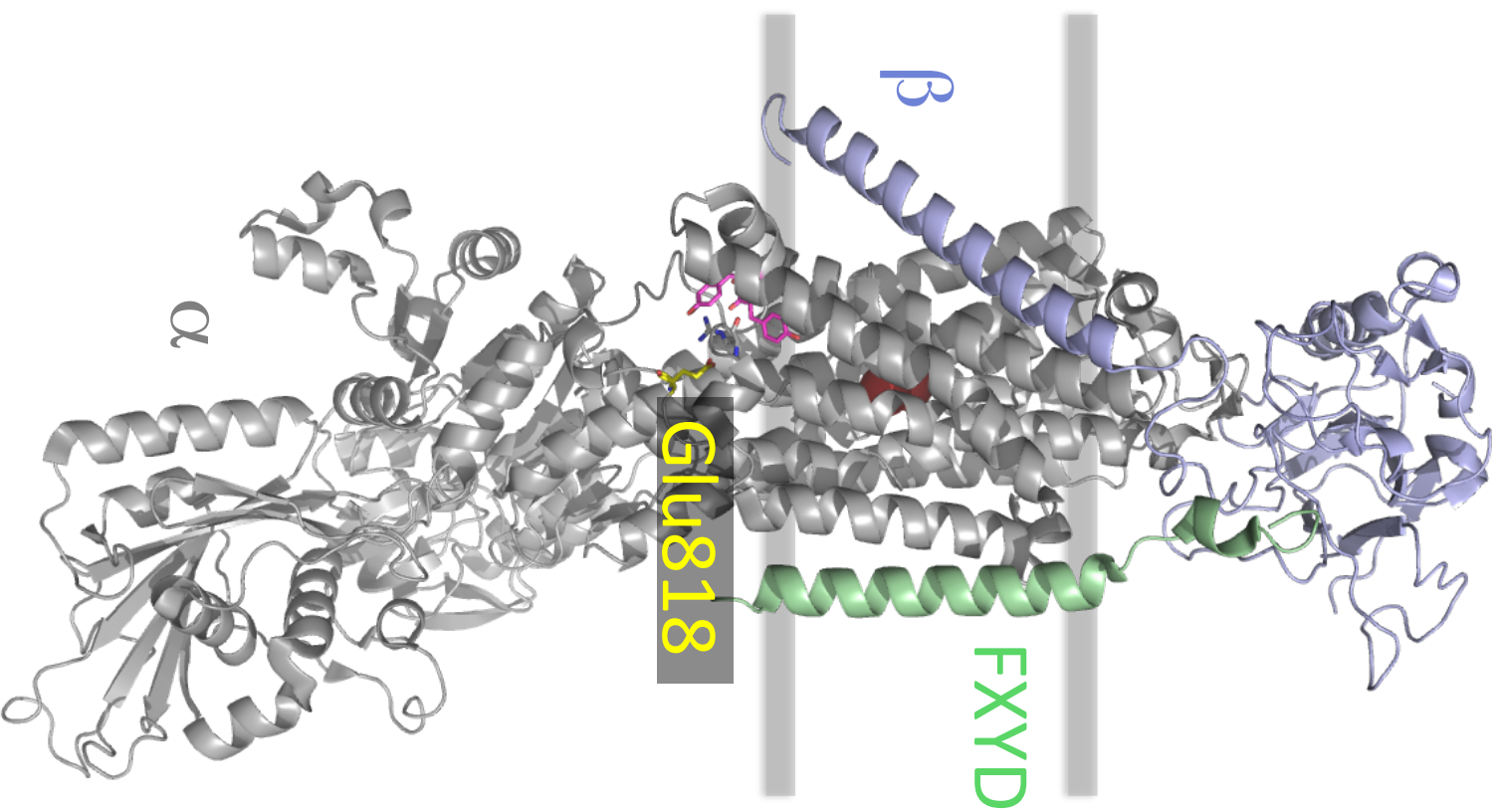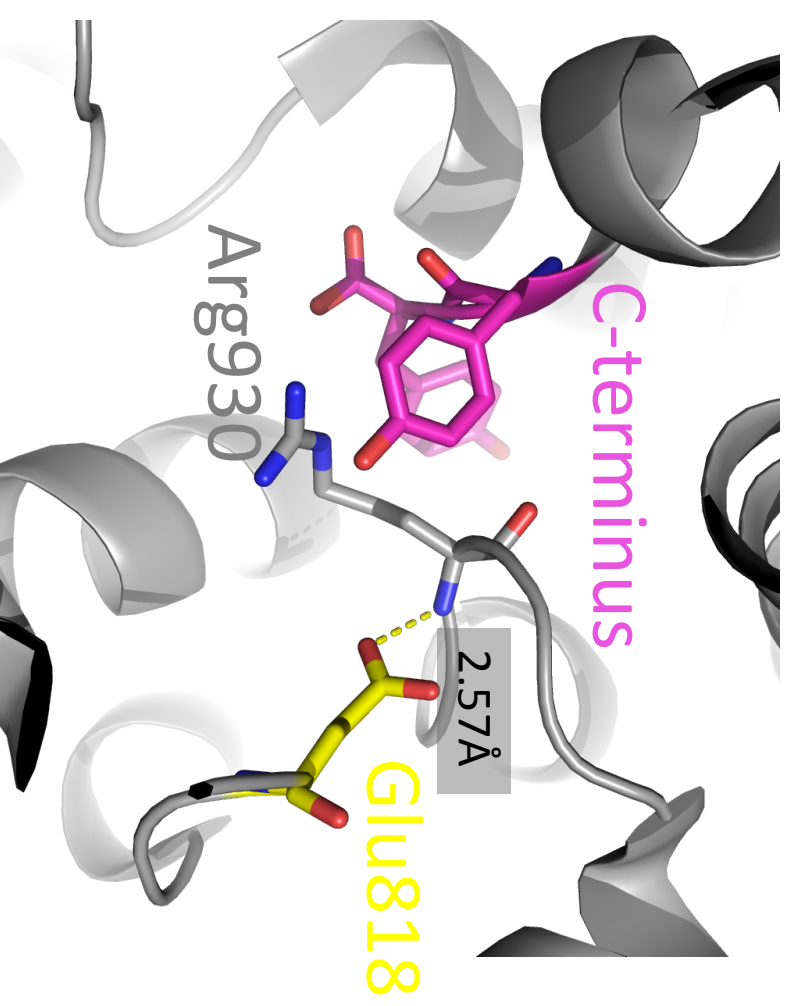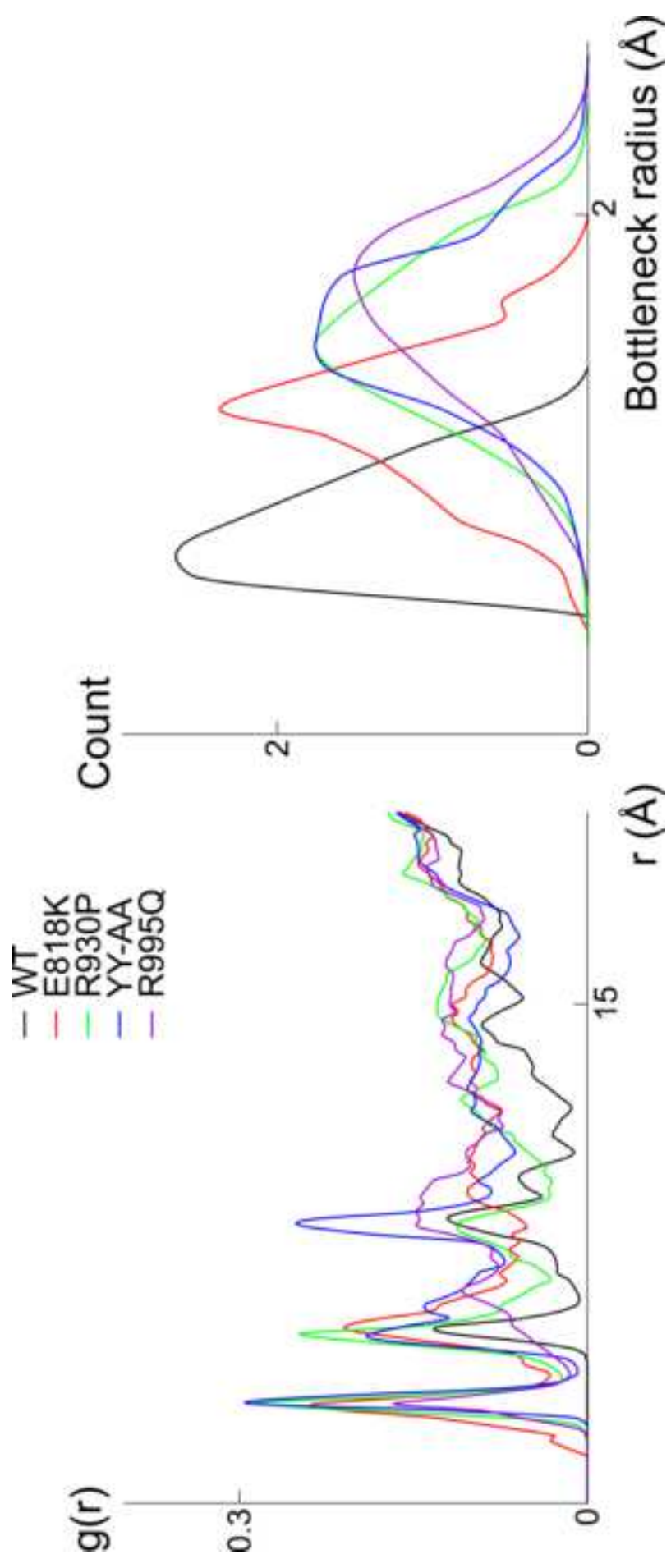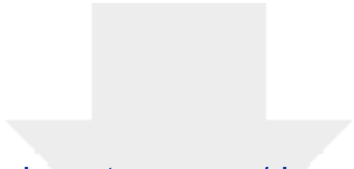
Click here to access/download
Supplementary Material
ESM_8.pdf
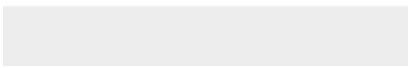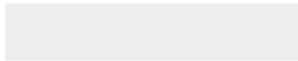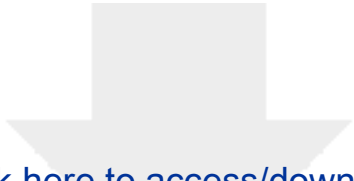
Click here to access/download
Supplementary Material
ESM_1.pdf
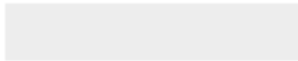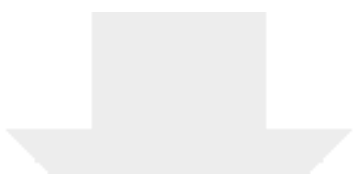
Click here to access/download
Supplementary Material
ESM_2.pdf
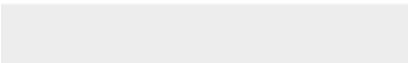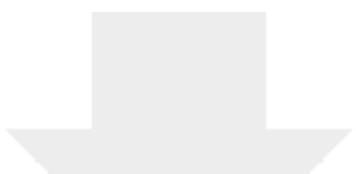
Click here to access/download
Supplementary Material
ESM_3.pdf
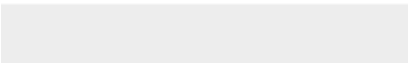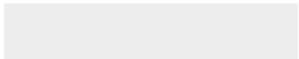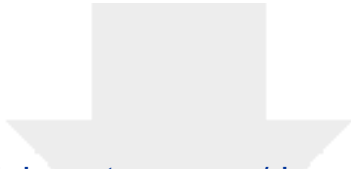
Click here to access/download
Supplementary Material
ESM_4.pdf
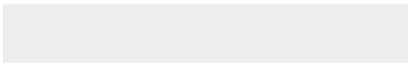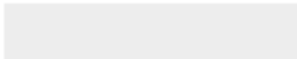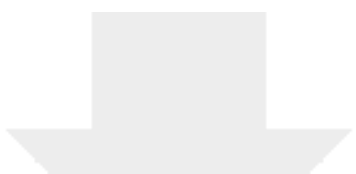
Click here to access/download
Supplementary Material
ESM_5.pdf
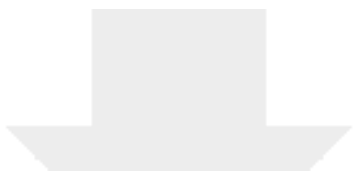
Click here to access/download
Supplementary Material
ESM_6.pdf

Click here to access/download
Supplementary Material
ESM_7.pdf